Analysis of the Footprint of Uncertainty of a Parallelogram Membership Function

Ahmed Abdul Ibrahim[1,2], Hai-bo ZHOU[2], Chao-long ZHANG[2], Ji-an DUAN[2]
[1]School of Mechanical and Electrical Engineering, Central South University, Changsha 410083, China.
[2]Ahmadu Bello University/ Department of Mechanical Engineering, Zaria 810222, Nigeria

E-mail: ahmedibrahim@csu.edu.cn, zhouhaiboo@csu.edu.cn, clzhang@csu.edu.cn, duanjiian@csu.edu.cn

Corresponding Author: Ahmed Abdul Ibrahim, ahmedibrahim@csu.edu.cn.

Received: 25-05-2022; **Accepted:** 23-08-2022; **Published:** 29-08-2022

***Abstract*:** The general effectiveness of fuzzy representation depends heavily on the membership functions. The best footprint of uncertainty for a specific fuzzy system is highly dependent on the nature of the problem that the fuzzy system is supposed to solve. As a result, a proper footprint of uncertainty size selection is needed to improve the fuzzy system's efficiency. This research intends to investigate the impact of a unique linear parallelogram membership function's footprint of uncertainty on nonlinear system modeling and control. The proposed type-2 membership function has a crisp membership degree at the end points of the footprint of uncertainty and uncertain values in-between. When dealing with data whose membership degree is certain at the boundary but uncertain in-between, the proposed membership function having its highest uncertainty at the midpoint of the membership function width is advantageous. Tuning the parameters of the proposed MF will provide a variety of triangular and quadrilateral footprints of uncertainty shapes that will better capture the training data's uncertainties. The gradient descent learning algorithm was used to tune the consequent parameters of the evaluated interval type-2 fuzzy system. The performance results demonstrated the effect of the footprint of uncertainty on linear parallelogram membership function-based fuzzy system's capability in prediction, identification, and control tasks.

Index Terms: Parallelogram membership function, footprint of uncertainty, interval type-2 fuzzy system, prediction, identification, control.

1. Introduction

Intelligent control methodologies are considered more successful when there is insufficient or uncertain knowledge available for modeling or control problems. The most widely used model-free approaches are artificial neural networks (ANN) and fuzzy systems. Zadeh's fuzzy set theory is a useful tool for describing subjective and inaccurate data in a variety of situations. According to studies, fuzzy systems are better at dealing with ambiguity than ANNs [1]. The adaptive neuro-fuzzy inference method, Takagi-Sugeno-Kang type recurrent fuzzy networks, fuzzy wavelet neural networks, and other approaches based on combining the ANN and the fuzzy system have become common [2]. These methods have been successfully applied in a variety of fields, including system approximation, control systems, pattern recognition, classification, medicine, chemistry, finance, and business.

In the field of system modeling and control, the Takagi-Sugeno (T-S) fuzzy system is the most widely used fuzzy system. Developing a T-S fuzzy model for system identification or control entails determining the structure as well as estimating the parameters of the model's antecedent and consequent parts [3, 4]. The type of membership function (MF) shape, number of MFs, how to reduce the computational cost, the number of rules needed, and so on are all considerations when designing fuzzy systems [5]. As a result, deciding which of these decisions is the most suitable is an important question for the designer to answer. It has also been claimed that there is no formal design process for fuzzy systems and that a fuzzy system's output is determined by the shape of its MF [6]. Type-2 fuzzy systems are more better at handling disruptions and uncertainties than type-1 fuzzy systems because the type-2 MF in type-2 systems is composed of an infinite number of type-1 MFs [7-13]. The key characteristic that distinguishes type-2 fuzzy systems from type-1 fuzzy systems is the footprint of uncertainty (FOU) [14]. The shape of the FOU fully defines the MFs and has a great effect on the approximation accuracy of the fuzzy system [15, 16].

A membership function is a curve that specifies a fuzzy set's feature by assigning a membership value or degree of membership to an element. In a closed unit interval [0, 1], each point in the space is mapped to a membership value. Researchers have presented various forms of MF in the related literature. Some MFs were introduced in [17], such as trapezoidal, triangular, Gaussian, and bell-shaped. The triangular MF first described by [18] is a subtype of the trapezoidal MF [19]. Diamond-shaped MFs with crisp values at the ends and unknown values in the center have been suggested in [20]. A nonlinear elliptical MF was proposed in [21, 22], with certain values on both ends of the support and the kernel and an uncertain value in the center. [23] proposed the beta fuzzy logic scheme. Semi-elliptic MF was proposed in [19]. A procedure for the generation of interval type-2 membership functions from data was proposed in [24].

Some data have a certain membership degree (MD) value at the boundary and uncertain MD in the middle. For example, six experts ranked 50 umbilical acid-base (UBA) assessments in terms of the likelihood of a patient suffering brain damage due to a lack of oxygen [25]. The relationship between an FLS decision and the type-2 MF FOU shape was studied. From the generated graph, it was observed that there is variation among the decisions and that the variation was greater at the middle range and less at the extreme edge. To collect all of the uncertain information from various experts, a more suitable type-2 MF for these types of data should have a certain MD at the ends (boundary) and an uncertain value in between. Unfortunately, the well-known Gaussian and triangular MFs do not have these properties. This motivated us to develop an MF that better represent the uncertain distribution.

In this paper, we present a novel linear parallelogram MF that has a certain MD at its ends and an uncertain MD in between. The proposed MF's FOU parameters are decoupled from the MF's center and width parameters, allowing us to explore the impact of the FOU parameters on the robustness in an interval type-2 fuzzy system. The proposed MF has fewer parameters than the diamond MF and is simpler than both the diamond and elliptical MFs. Similar to other linear MFs, our parallelogram MF cannot be optimized using derivative base optimizers.

The rest of this paper is presented as follows: The fuzzy type-2 system and parallelogram MF are briefly described in section 2. Prediction and control simulation results are presented in Section 3. Experimental validation of simulation findings is presented in section 4. The paper concludes with Section 5.

2. Type-2 Fuzzy System

Systems built on a type-2 fuzzy set are known as type-2 fuzzy systems [26]. The fuzzy IF-THEN rules of the type-2 fuzzy system contain type-2 fuzzy set [27]. The uncertain membership function (MF) of the type-2 fuzzy set, which creates the footprint of uncertainty, distinguishes it from the type-1 fuzzy set (FOU).

2.1. Structure of an Interval Type-2 Fuzzy System

In this paper, the antecedent interval type-2 and consequent type zero (A2-CO) fuzzy system is adopted. It consists of type-2 MFs in the premise part and crisp values in the consequent part. Their rules are as in Eq. (1).

IF x_1 is A_1^j , x_2 is A_2^j , …, and, x_m is A_m^j, THEN $y_j = \sum_{i=1}^{m} ar_{ij} x_i + b_j$ (1)

where $x_1, x_2, \ldots, x_m$ are the input variables with (i = 1, 2,…, m), and the output variables are y_j $with$ (j = 1,2,…,n); A_m^j is a type-2 fuzzy set of the j^{th} rule of the i^{th} input; ar_{ij} and b_j are resulting parameters of the network.

The purpose of the fuzzy system is to segment the input space into fuzzy domains in the antecedent section of the rule so that each class has a corresponding consequent component. The membership functions of an interval type-2 fuzzy system are represented by an upper and lower MF, which are, respectively, written as $\bar{\mu}(x)$ and $\underline{\mu}(x)$. The "min" or "prod" t-norm is typically the implication operator of the inference engine. The product t-norm given by Eq. (2 & 3) is used in our model as recommended by [28].

$$\underline{f} = \underline{\mu}_{\tilde{A}_1}(x_1) * \underline{\mu}_{\tilde{A}_2}(x_2) * \ldots * \underline{\mu}_{\tilde{A}_n}(x_n) \quad (2)$$

$$\bar{f} = \bar{\mu}_{\tilde{A}_1}(x_1) * \bar{\mu}_{\tilde{A}_2}(x_2) * \ldots * \bar{\mu}_{\tilde{A}_n}(x_n) \quad (3)$$

The format of the inference block outputs is fuzzy interval type-2. The type of reducer block converts it to a fuzzy type-1, which is then de-fuzzified to a crisp value at the defuzzification block. The fuzzy system's output can be calculated using [29],

$$Y = \frac{q\sum_{j=1}^{N} \underline{f}_j y_j}{\sum_{j=1}^{N} \underline{f}_j} + \frac{(1-q)\sum_{j=1}^{N} \overline{f}_j y_j}{\sum_{j=1}^{N} \overline{f}_j} \tag{4}$$

$$y_j = \sum_{i=1}^{m} ar_{ij} x_i + b_j \qquad i = 1,2, \ldots, n \quad j = 1,2, \ldots, m$$

"*q"* is a design parameter that determines the contribution of the upper and lower values to the final output.

2.2. Parallelogram Membership Function

This paper introduces a novel linear parallelogram MF that can be transformed into different type-1 and interval type-2 MF shapes. It is obtained by modification of the triangular MF by the introduction of two parameters ($a_1$anda_2) that define the shape and width of the FOU. It is similar to the diamond-shaped MF but with a simpler and smaller number of parameters that define the function. "a_1"and "a_2" are the parameters responsible for the shape of the FOU are decoupled from the parameters for the center (*c*) and width (*d*), as will be shortly explained in detail. This allows us to investigate the impact of the FOU parameters on the type-2 fuzzy system's approximation ability. Our proposed MF and the elliptic MF have this advantage over the triangular and Gaussian MFs. The mathematical expression of the upper and lower parallelogram MF are,

$$\overline{\mu}_i = \begin{cases} a_1\left(1-\left|\frac{x-c_1}{d}\right|\right) & if \quad c-2d \le x \prec c-d \\ a_1 + b_1\left(1-\left|\frac{x-c}{d}\right|\right) & if \quad c-d \le x \prec c+d \\ a_1\left(1-\left|\frac{x-c_2}{d}\right|\right) & if \quad c+d \le x \prec c+2d \\ 0 & else \end{cases} \tag{5}$$

$$\underline{\mu}_i = \begin{cases} a_2\left(1-\left|\frac{x-c_1}{d}\right|\right) & if \quad c-2d \le x \le c-d \\ a_2 + b_2\left(1-\left|\frac{x-c}{d}\right|\right) & if \quad c-d \le x \le c+d \\ a_2\left(1-\left|\frac{x-c_2}{d}\right|\right) & if \quad x \le c+2d \\ 0 & else \end{cases} \tag{6}$$

where $c_1 = c - d$, $c_2 = c + d$, $b_1 = 1 - a_1$, $b_2 = 1 - a_2$, hence only three parameters are required to describe the MF ($\bar{\mu}_i$) which are; $c, d,$ and a_1, while the parameters for the lower MF ($\underline{\mu}_i$) are; $c, d,$ and a_2.

2.3 Formulation of Footprint of Uncertainty Shapes using the Parallelogram Membership Function

As can be seen in Figs. 1-3, the upper and lower MF ($\bar{\mu}_i$ and $\underline{\mu}_i$) are defined all through the universe of discourse. Both a_1 and a_2 can take values between zero and one. When a_1 and a_2 are used as complementary parameters ($a_2 = 1 - a_1$), a type-2 parallelogram MF will be formed except at $a_1 = a_2 = 0.5$ where it transforms into a type-1 triangular MF, as shown in Fig. 1. The width of the uncertainty is determined by the value of a_1 and a_2. When

$a_1 = a_2$, a type-1 MF will be formed whose shape depends on the values of a_1 and a_2. The shapes vary from trapezoidal at $a_1 = a_2 = 1$, to pentagonal at $a_1 = a_2 < 1$, and then triangular at $a_1 = a_2 = 0$ as shown in Fig.2 (a, b, and c) respectively. When $a_1 \neq a_2$ and are not complimentary, a type-2 quadrilateral MF is formed except where $a_1 = 0.5$ or $a_2 = 0.5$, which forms a type-2 triangular MF. Some of the cases for $a_1 \neq a_2$ are shown in Fig. 3. These show the proposed MF's ability to flexibly transform to various shapes to appropriately represent the uncertainties.

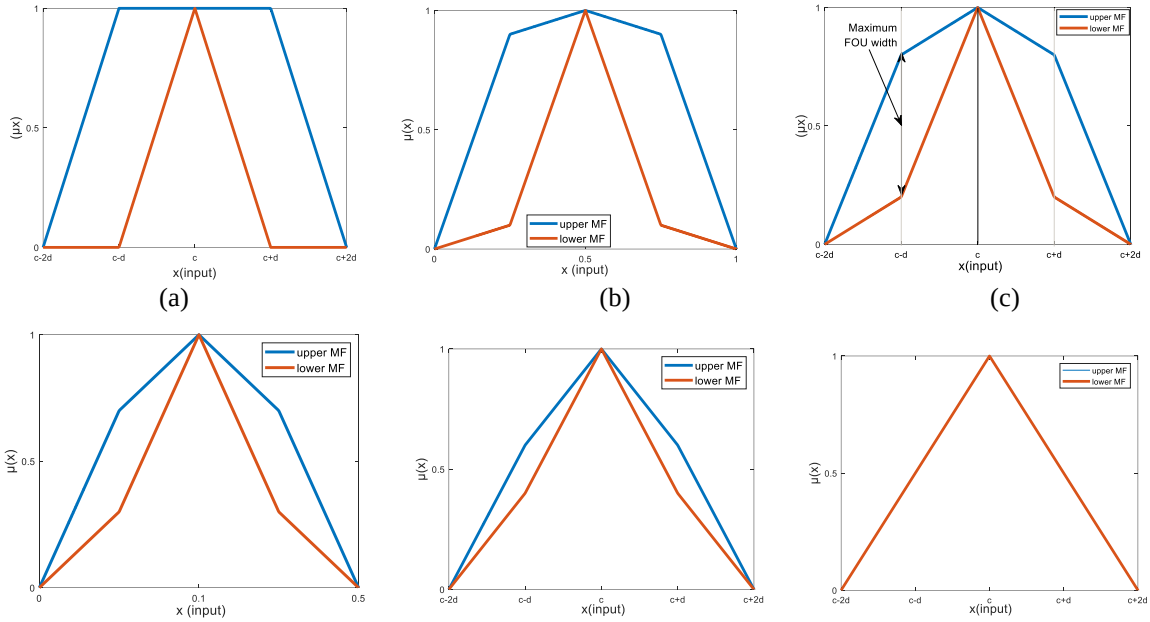

Fig. 1. Shapes of the proposed type-2 parallelogram MF with different values of *a1* and *a2*

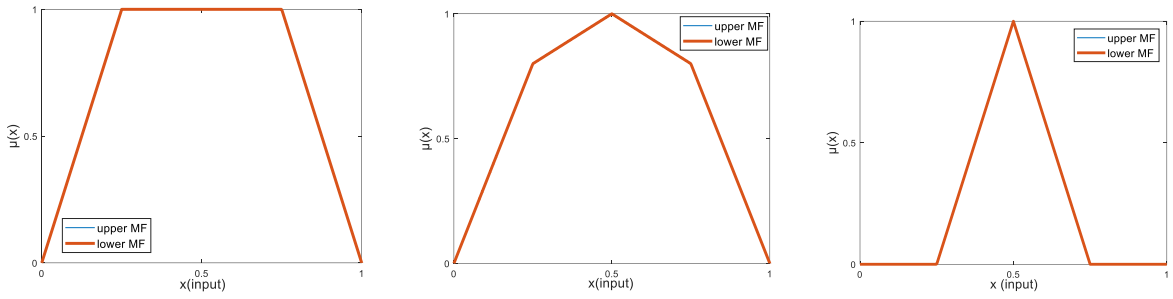

Fig. 2. Shapes of the transformed type-1 MF when; (a) $a_1 = a_2 = 1$, (b) $a_1 = a_2 < 1$, (c) $a_1 = a_2 = 0$

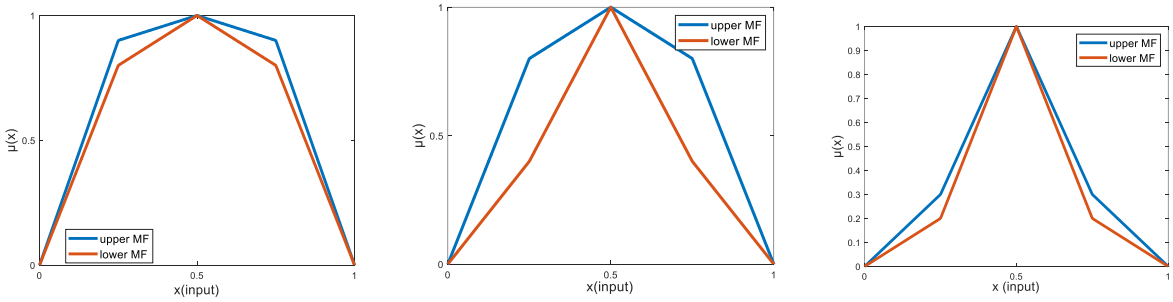

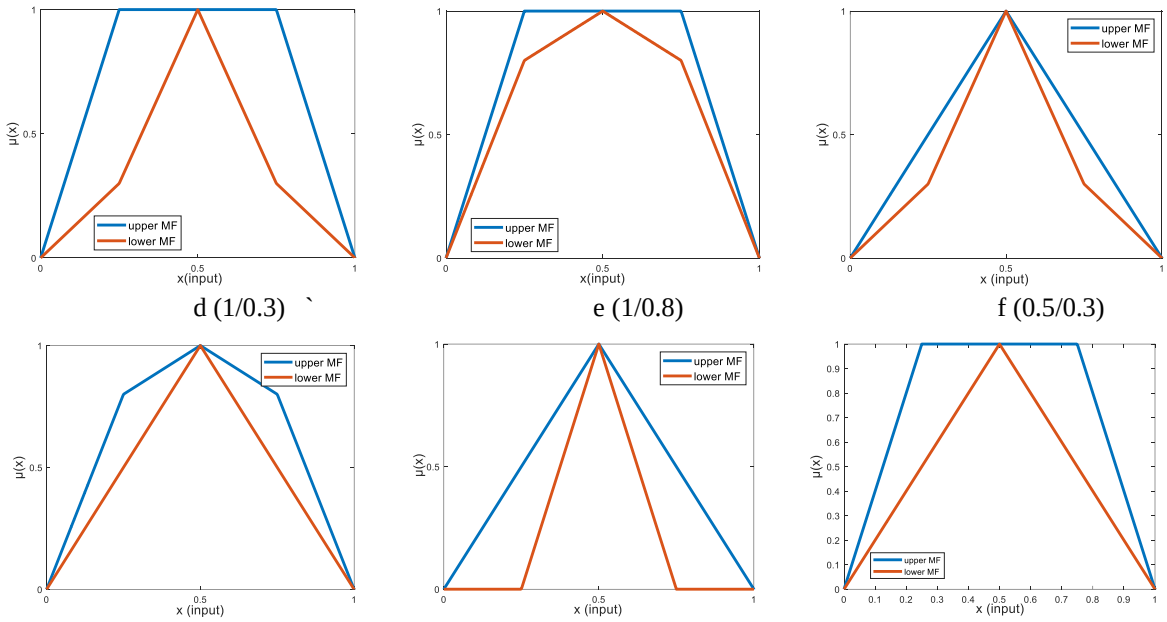

d (1/0.3) ` e (1/0.8) f (0.5/0.3)

g (0.8/0.5) h (0.5/0) i (1/0.5)

Fig. 3. Other possible FOU shape for difference parameters (a_1/a_2) values of the parallelogram MF.

2.4. Determination of System Stability and Parameters

The crucial element of fuzzy system design is determining appropriate parameters for both the antecedent and consequent parts of the fuzzy system. We chose fixed sets of parameters for the MF in sections 3.1, 3.2, and 4.1 because our focus is on the effect of the FOU parameters on the output of the fuzzy system. To achieve stability, the consequent parameters were adjusted using the gradient descent algorithm [2]. The stability condition to be satisfied is given by

$$\Delta E = \left[E\left(t+1\right) - E\left(t\right) \right] \leq 0 \tag{7}$$

The cost function is given by,

$$E = \frac{1}{2}\left(y_d - y\right)^2 \tag{8}$$

where y_d and y represent the desired and current output of the network.
The consequent parameter update using gradient descent algorithm is as follows,

$$ar_{ij}\left(t+1\right) = ar_{ij}\left(t\right) - \gamma \frac{\partial E}{\partial ar_{ij}} \tag{9}$$

$$b_j\left(t+1\right) = b_j\left(t\right) - \gamma \frac{\partial E}{\partial b_j} \tag{10}$$

Where m_{ij} represent the antecedent parameters (mean/width and STD), ar_{ij} and b_j represent the consequent parameters of the fuzzy system, γ represent the learning rate. Using IF/THEN rules, the algorithm adjusts the parameters to satisfy the stability condition of Eq. 7, hence making the cost function convergent.
The derivatives in Eq. 9 & 10 are determined as follows,

$$\frac{\partial E}{\partial ar_{ij}} = \frac{\partial E}{\partial u}\frac{\partial u}{\partial u_j}\frac{\partial u_j}{\partial ar_{ij}} \tag{11}$$

$$\frac{\partial E}{\partial b_j} = \frac{\partial E}{\partial u}\frac{\partial u}{\partial u_j}\frac{\partial u_j}{\partial b_j} \tag{12}$$

The derivatives in Eq. 11, and 12 are determined as follows,

$$\frac{\partial E}{\partial u} = y(t) - y_d(t) \tag{13}$$

$$\frac{\partial u}{\partial u_j} = 1$$

$$\frac{\partial u_j}{\partial ar_{ij}} = r_j x_i$$

$$\frac{\partial u_j}{\partial b_j} = r_j$$

3. Simulation Studies

This section examines the impact of the proposed parallelogram MF's FOU parameters (a_1 and a_2) on the output of the interval type-2 fuzzy system (IT2FS). In order to attain the best values, parameters are typically modified using optimization techniques, or some constant values are selected by professionals [1]. For the analysis in sections 3.1 and 3.2, we chose some constant values to observe the changes in IT2FS output for each set of parameters. There are six sets of FOU parameters (a_1 and a_2): 1 & 0, 0.9 & 0.1, 0.8 & 0.2, 0.7 & 0.3, 0.6 & 0.4, and 0.5 & 0.5 selected for the analysis. Fig. 1 depicts their MF forms. Except for a_1= 0.5 and a_2= 0.5, which is a type-1 triangular MF, all of the parameters are type-2 parallelogram MFs. In all the analyses, two MFs were used for each input. The gradient descent algorithm was used to tune the parameters of the IT2FS's consequent components. For prediction and control analysis, the chaotic Mackey-Glass time series and the 3 PRS parallel robot were used, respectively. The MATLAB R2018a software was used for all of the model's training and testing procedures. The accuracy measure is based on the testing RMSE given by Eq. (14). All the algorithms aim to minimize the RMSE. The generated data was corrupted with noise at various levels for robustness analysis using Eq. (15).

$$RMSE = \sqrt{1/K\sum_{i=1}^{k}\left(y(k) - y_N(k)\right)^2} \tag{14}$$

$$SNR = 20\log_{10}\left(\frac{\sigma_s}{\sigma_n}\right) \tag{15}$$

Where $y_N(k)$ denotes the model output, $y(k)$ represents the system output, k represents the number of samples, σ_s represents the standard deviation of the data, and σ_n represents the standard deviation of the noise.

3.1. Prediction of the Chaotic Mackey-Glass Time Series

The Mackey-Glass time series [23] was used to assess the prediction accuracy of the IT2FS with our parallelogram MF. The FOU parameters are adjusted as previously mentioned. The Mackey-Glass time series problem is a well-known benchmark problem, which is expressed as:

$$\frac{dx(t)}{dt} = \frac{0.2x(t-\tau)}{1+x^{10}(t-\tau)} - 0.x(t) \tag{16}$$

Where τ = 17, the initial value was $x(0)$ = 1.2, and the input-out format was $[x(t-24), x(t-18), x(t-12), x(t-6); x(t)]$. From t = 124 s to t = 1123 s, the first 500 patterns we generated were used in the training phase, while the remaining 500 patterns were used in the validation process.

Table 1 shows that by using both the uncorrupted and corrupted data at various noise levels, the parameter (a_1=1, $a_2 = 0$) had the highest RMSE and thus the least accuracy. Fig 4 shows that the RMSE decreases as the FOU size increases until it reaches the FOU with the lowest RMSE, after which it begins to increase. All of the noise levels studied showed a similar trend. This suggests that having a wider than required FOU will reduce accuracy. The type-1 MF parameters a_1=0.5 and $a_2 = 0.5$ did not demonstrate any superiority in any of the noise levels tested, confirming the type-1 MF's inability to manage uncertainties better than the type-2 MF. Different FOU parameters performed better at different noise levels, indicating that the appropriate parameters are data-dependent. As a result, using expert knowledge or optimization techniques can go a long way toward determining the best parameters for a given data set. The generally low RMSE performance demonstrates the effectiveness of the proposed MF in handling noisy data.

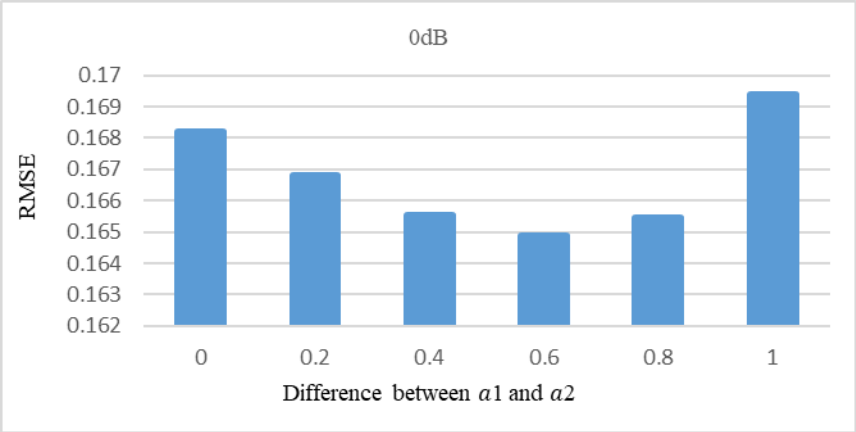

Fig. 4. Width of the FOU versus accuracy RMSE

Table 1: Prediction accuracy for each of the FOU parameters with respect to noise level

	FOU parameters (a_1/a_2)					
SNR	1/0	0.9/0.1	0.8/0.2	0.7/0.3	0.6/0.4	0.5/0.5
uncorrupted	0.03082	0.02963	0.025	**0.02496**	0.02812	0.03042
0 dB	0.16937	0.16546	**0.16488**	0.16555	0.16679	0.1682
2 dB	0.159	0.15514	0.1533	**0.15328**	0.15415	0.15518
4 dB	0.1355	0.13273	0.13076	**0.13027**	0.13086	0.13212
6 dB	0.11909	**0.10746**	0.10775	0.11006	0.11323	0.11649
8 dB	0.10897	**0.09865**	0.09858	0.10123	0.10466	0.10829
10 dB	0.09314	0.08402	**0.08265**	0.08375	0.08591	0.0884

3.2. 3-PRS Parallel Robot Control

The 3-PRS parallel robot is used in integrated circuit manufacturing, precision machining and assembly, MEMS packaging, biochip preparation, and other fields. In this section, IT2FS was used to control a 3-PRS parallel robot model using the novel membership function. Each pair of the FOU parameters (a_1 and a_2) 1 & 0, 0.9 & 0.1, 0.8 & 0.2, 0.7 & 0.3, 0.6 & 0.4, and 0.5 & 0.5 were used to construct the IT2FS, and their effects on the IT2FS performance were evaluated using the integral of the squared error (ISE), integral absolute error (IAE), and integral of the product of time and absolute error (ITAE) [30]. The simulation was run for 120 seconds with a unit phase input as a reference signal. Fig. 5 depicts the control setup.

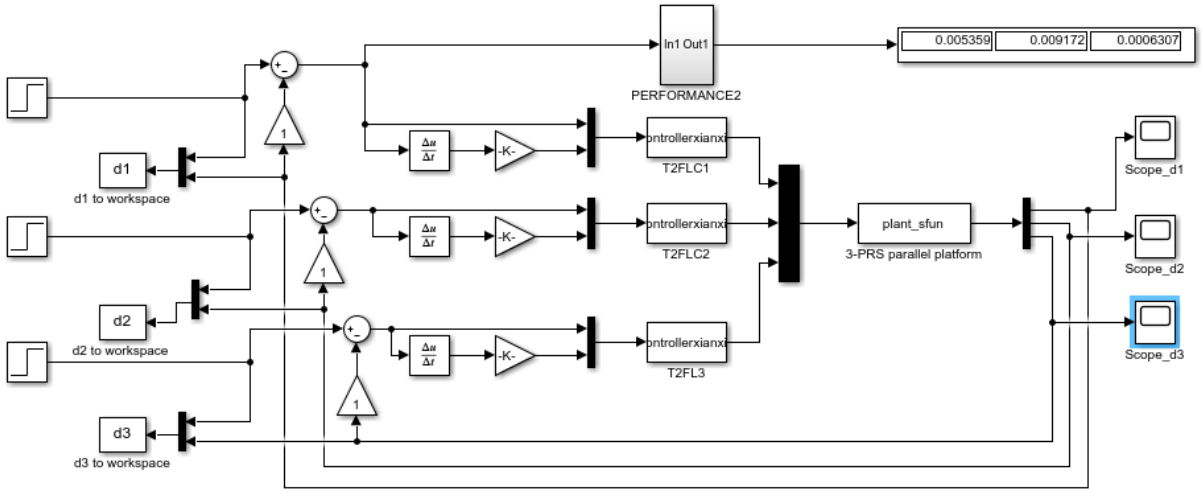

Fig. 5. The 3-PRS robot control setup

Figs. 6, 7, and 8 depict the accuracy of the IT2FSs in terms of ISE, IAE, and ITAE, respectively, under external noise-free conditions. The ISE result in Fig. 7 shows that as the FOU size (difference between $a_1$and a_2) increases, the controller's accuracy in terms of ISE increases, with the parameter (a_1=1, $a_2 = 0$) having the lowest ISE. This demonstrates the FOU's efficacy in lowering the ISE. The parameters (a_1=0.8, $a_2 = 0.2$) in Fig. 9 had the lowest ITAE, contrary to the ISE result. This demonstrates that the appropriate FOU parameter for a controller is determined by the performance criteria being considered. As can be seen in Figs. 7, 8, and 9, the low RMSE results also indicate that some or all of the type-2 based systems outperformed their type-1 counterparts (a_1=0.5 $a_2 = 0.5$).

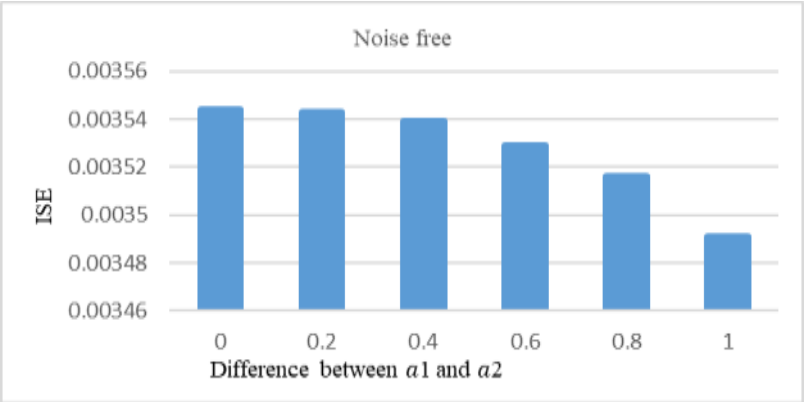

Fig. 6. Width of the FOU versus the integral square error (ISE)

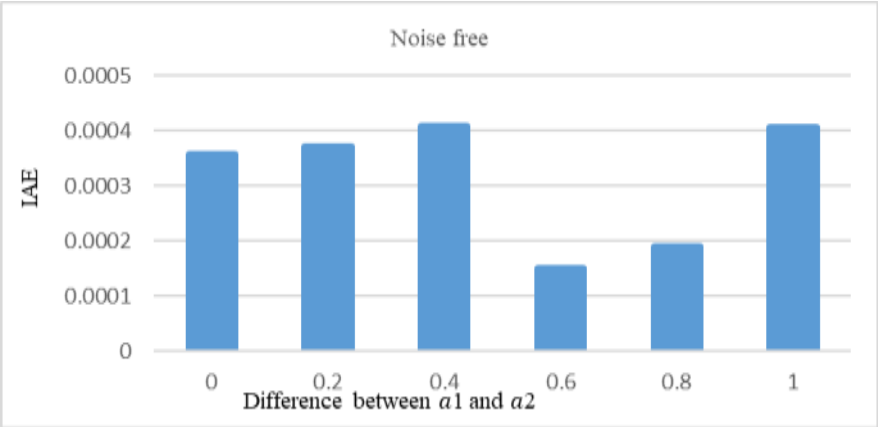

Fig. 7. Width of the FOU versus the integral absolute error (IAE)

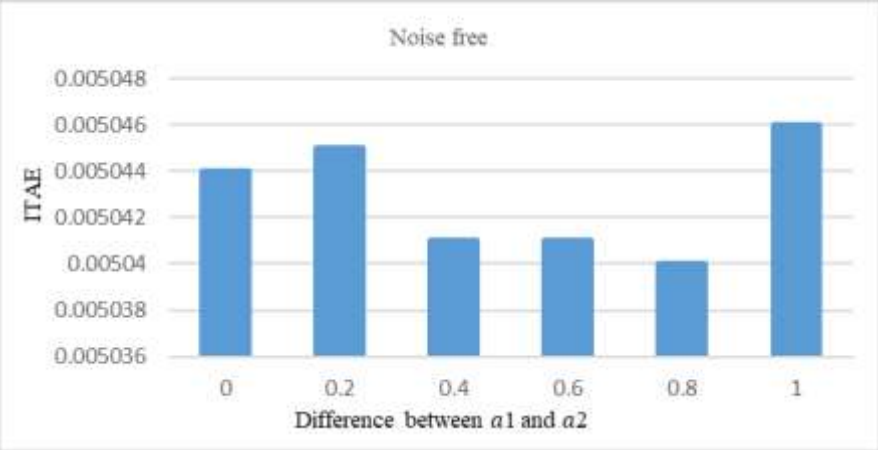

Fig. 8. Width of the FOU versus integral time absolute error (ITAE)

External noise at intervals of [-0.1; 0.1] was added to the 3-PRS robot's output to determine the robustness of the IT2FSs. The simulation was performed ten times, and an average performance result was calculated. Figs. 9, 10, and 11 display the efficiency of the IT2FSs under external noise conditions for the ISE, IAE, and ITAE, respectively. In all performance parameters, some type-2 MFs ($a_1 - a_2 \geq 0$) based controllers outperformed the type-1 MF ($a_1 - a_2 = 0$), just as they did in the noise-free condition. The performance relationship of the different FOU sizes is inconsistent throughout the three performance criteria, which also shows that the ideal FOU size is determined by the performance criterion being considered.

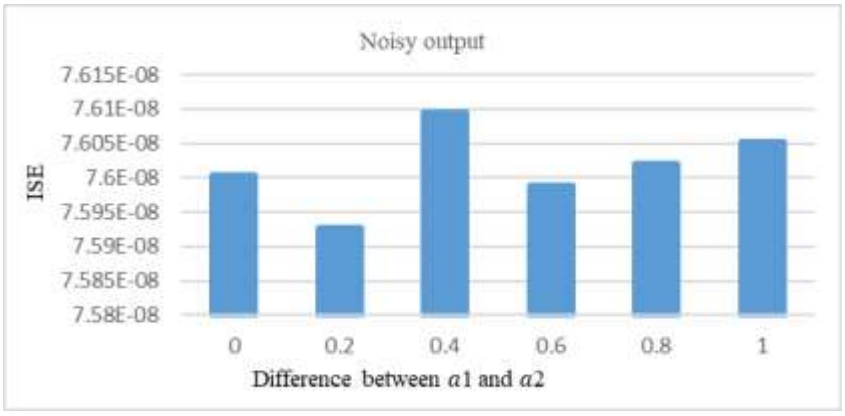

Fig. 9. Width of the FOU versus integral square error (ISE)

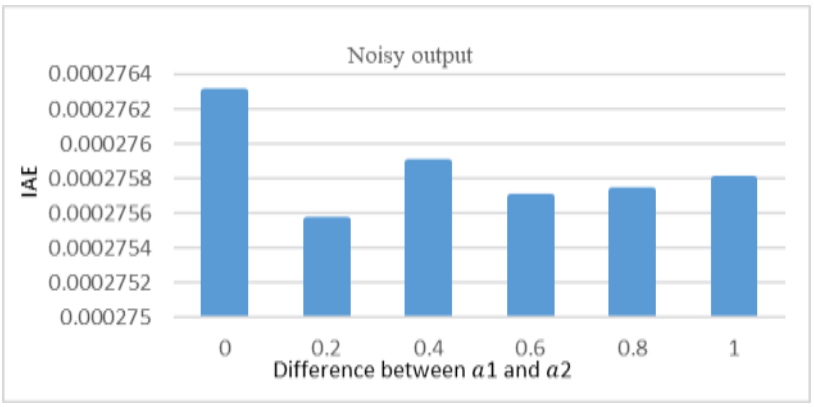

Fig. 10. Width of the FOU versus integral absolute error (IAE)

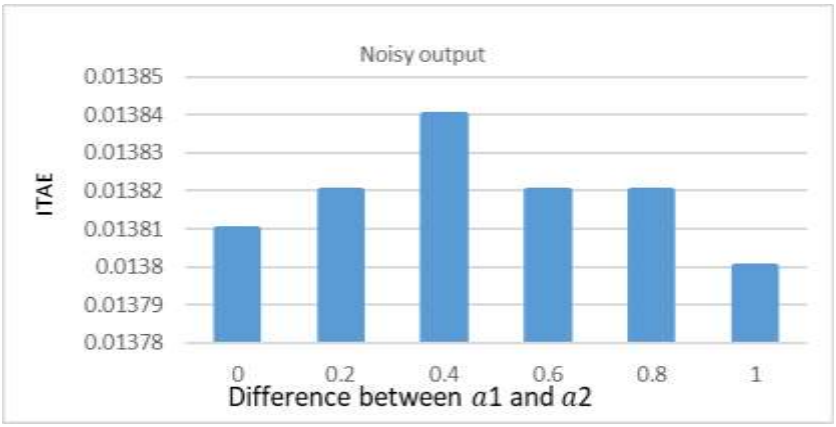

Fig. 11. Width of the FOU versus integral time absolute error (ITAE)

4. Experimental Evaluation of the Parallelogram Membership Function

This section experimentally examines the impact of the proposed parallelogram MF's FOU parameters (a_1 and a_2) on the output of the interval type-2 fuzzy system (IT2FS). For the analysis in section 4.1, we chose some constant values to observe the changes in IT2FS output for each set of parameters. There are six sets of FOU parameters (a_1 and a_2): 1 &

0, 0.9 & 0.1, 0.8 & 0.2, 0.7 & 0.3, 0.6 & 0.4, and 0.5 & 0.5 selected for the analysis. Except for a_1= 0.5 and a_2= 0.5, which is a type-1 triangular MF, all of the parameters are type-2 parallelogram MFs. In all the analyses, two MFs were used for each input. The gradient descent algorithm was used to tune the parameters of the IT2FS's consequent components. The MATLAB R2018a software was used for all of the model's training and testing procedures. The accuracy measure is based on the testing RMSE given by Eq. (14). All the algorithms aim to minimize the RMSE. The generated data was corrupted with noise at various levels for robustness analysis using Eq. (15).

4.1. 6-PSS Complaint Parallel Robot Setup

An important part of optoelectronic packaging is the 6-PSS parallel robot shown in Fig. 12. This robot changes the orientation of optical fibers to achieve microscale high-precision coupling [31]. The inverse kinematic action of the parallel robot was determined using the top moving platform (surge, sway, heave, roll, pitch, and yaw). The output, however, was the measured corresponding measured lengths of the six legs (L, 1,2,3,4,5, and 6). To determine how far the top platform must be moved by the six legs to obtain the required position, the inverse kinematic model was used. We generated 1134 input-output data pairs, out of which 567 were used for training and the remaining 567 are used for testing using the 6-PSS parallel robot. We trained the IT2FSs containing the suggested MF with various FOU parameters to show the potential of the proposed parallelogram based IT2FS. For all models, we utilized 100 training epochs and two MFs for each input.

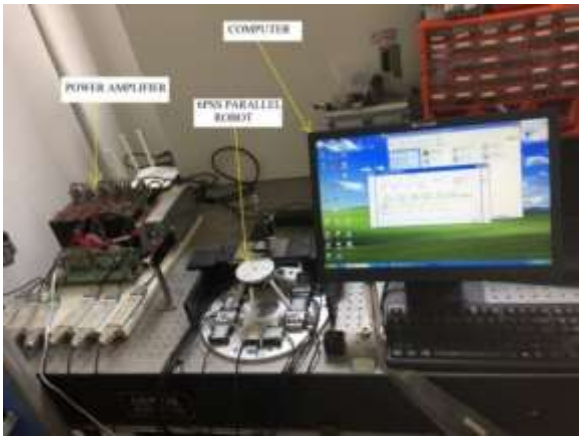

Fig. 12. Running setup of 6-PSS parallel robot.

4.2. 6-PSS Complaint Parallel Robot Identification

In the field Though the parameters a_1=0.7, $a_2 = 0$.3 had the best overall performance (lowest RMSE) at all the noise levels, as shown in Tables 2 to 5, the parameters a_1=0.8, $a_2 = 0$.2 and a_1=0.6, $a_2 = 0$.4 had the best performance for Leg 3 and 5, respectively, as shown in Table 2 to 4. This confirms that the appropriate FOU parameters are determined by the nature of the data. As a result, using expert knowledge or optimization methods to arrive at the best parameter values is strongly advised. As shown in Fig. 13, the accuracy improves as the FOU size increases from a_1=0.5, $a_2 = 0.5$, which is a type-1 fuzzy set, to the type-2 fuzzy set parameter with the highest accuracy, and then begins to decrease as the FOU size further increases. All the noise levels yielded a similar pattern. The parameter a_1=1, $a_2 = 0$, which is the largest FOU size, had the lowest accuracy, indicating that using a larger FOU size than needed reduces accuracy.

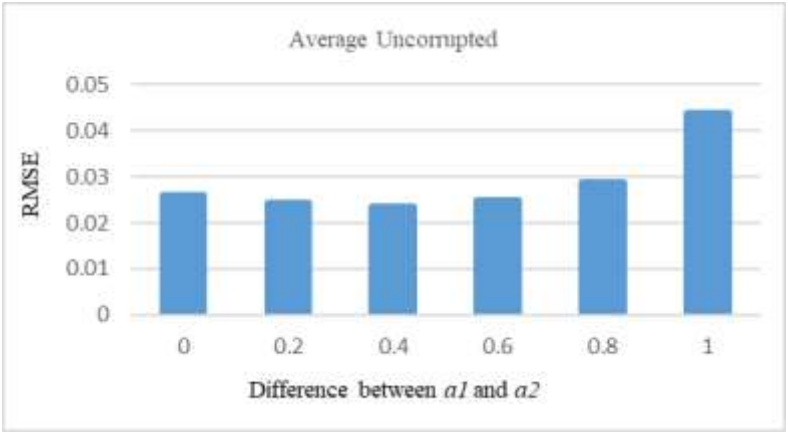

Fig. 13 Width of the FOU versus accuracy RMSE

Table 2: Identification accuracy of the FOU parameters using uncorrupted data.

	FOU parameters (a_1 and a_2)					
Leg No.	1/0	0.9/0.1	0.8/0.2	0.7/0.3	0.6/0.4	0.5/0.5
L 1	0.0509	0.0307	0.0254	**0.0221**	0.0224	0.0252
L 2	0.0393	0.0288	0.0258	**0.0251**	0.0258	0.0267
L 3	0.0289	0.0191	**0.017**	0.0171	0.0181	0.0186
L 4	0.0464	0.0345	0.0308	**0.0295**	0.0307	0.0318
L 5	0.0397	0.0284	0.0253	0.0227	**0.0225**	0.0234
L 6	0.0573	0.0316	0.0257	**0.024**	0.0271	0.031
Average	0.0438	0.0289	0.0250	**0.0234**	0.0244	0.0261

Table 3: Identification accuracy of the FOU parameters using 20 dB

	FOU parameters (a_1 and a_2)					
Leg No.	1/0	0.9/0.1	0.8/0.2	0.7/0.3	0.6/0.4	0.5/0.5
L 1	0.06309	0.03254	0.02585	**0.02178**	0.02205	0.03685
L 2	0.04717	0.02857	0.02507	**0.02414**	0.02507	0.02597
L 3	0.03813	0.02096	**0.01838**	0.01851	0.01978	0.02055
L 4	0.05212	0.03539	0.03104	**0.02982**	0.03112	0.03238
L 5	0.04329	0.02967	0.02544	0.02256	**0.0224**	0.02325
L 6	0.05841	0.0325	0.02625	**0.02476**	0.02803	0.03222
Average	0.0504	0.0299	0.0253	**0.0236**	0.0247	0.0285

Table 4: Identification accuracy of the FOU parameters using 15 dB

	FOU parameters (a_1 and a_2)					
Leg No.	1/0	0.9/0.1	0.8/0.2	0.7/0.3	0.6/0.4	0.5/0.5
L 1	0.06129	0.03261	0.02584	**0.02239**	0.02337	0.02633
L 2	0.04298	0.02919	0.02556	**0.02491**	0.02609	0.02705
L 3	0.03598	0.02081	**0.0179**	0.01800	0.01918	0.01979
L 4	0.05804	0.03581	0.03019	**0.02900**	0.03081	0.03242
L 5	0.06011	0.03207	0.02612	0.02267	**0.02230**	0.02324
L 6	0.0667	0.03508	0.02818	**0.02649**	0.02922	0.03314
Average	0.0542	0.0309	0.0256	**0.0239**	0.0252	0.0270

Table 5: Identification accuracy of the FOU parameters using 10dB

	FOU parameters (a_1 and a_2)					
Leg No.	1/0	0.9/0.1	0.8/0.2	0.7/0.3	0.6/0.4	0.5/0.5
L 1	0.06988	0.0348	0.02737	**0.02534**	0.02847	0.03173
L 2	0.04582	0.02983	0.02594	**0.02567**	0.02732	0.02834
L 3	0.04290	0.02556	0.02126	**0.02122**	0.02252	0.02319
L 4	0.06577	0.04059	0.03636	**0.03632**	0.03942	0.04161
L 5	0.06795	0.03654	0.02858	**0.0247**	0.02509	0.02659
L 6	0.062	0.0333	0.02722	**0.02632**	0.03071	0.03458
Average	0.0591	0.0334	0.0278	**0.0266**	0.0289	0.0310

5. Conclusion

We presented a novel linear parallelogram type-2 MF with crisp endpoints and uncertain values in between. The parameters that influence the FOU shape in our proposed MF are separated from those that regulate the MF's width and center. This allowed for the examination of the impacts of FOU settings on the noise reduction capacity of the IT2FS while employing the suggested MF. The simulation outcome demonstrates the innovative MF's capacity to deal with uncertainty. The data generated experimentally from a 6-PSS parallel robot was also utilized to support the simulation findings. The limitation of the linear parallelogram MF, just like all linear MFs is the inability to optimize its parameters using derivative-based optimizers. Further study on the proposed MF's area of suitability can be conducted. A performance comparison of the proposed MF with other existing MFs can also be conducted.

Acknowledgment

The National Key R&D Program of China [grant numbers 2017YFB1104800] and the National Natural Science Foundation of China [grant numbers 51975590] each provided grants in support of this work.

References

[1] Mendel, Jerry M. "Uncertain rule-based fuzzy systems." Introduction and new directions 684 (2017).

[2] Khanesar, Mojtaba Ahmadieh, Erdal Kayacan, Mohammad Teshnehlab, and Okyay Kaynak. "Analysis of the noise reduction property of type-2 fuzzy logic systems using a novel type-2 membership function." IEEE Transactions on Systems, Man, and Cybernetics, Part B (Cybernetics) 41, no. 5 (2011): 1395-1406.

[3] Zarandi, MH Fazel, Mohammad Reza Faraji, and M. Karbasian. "Interval type-2 fuzzy expert system for prediction of carbon monoxide concentration in mega-cities." Applied soft computing 12, no. 1 (2012): 291-301.

[4] Su, Zhi-gang, Pei-hong Wang, Jiong Shen, Yu-fei Zhang, and Lu Chen. "Convenient T–S fuzzy model with enhanced performance using a novel swarm intelligent fuzzy clustering technique." Journal of Process Control 22, no. 1 (2012): 108-124.

[5] Wu, Dongrui. "Twelve considerations in choosing between Gaussian and trapezoidal membership functions in interval type-2 fuzzy logic controllers." In 2012 IEEE International conference on fuzzy systems, pp. 1-8. IEEE, 2012.

[6] Šaletić, Dragan Z., and Uroš Popović. "Design of fuzzy controllers based on automatic selection of membership functions shapes." In 10th Symposium on Neural Network Applications in Electrical Engineering, pp. 131-136. IEEE, 2010.

[7] Raj, Ritu, and B. M. Mohan. "General structure of interval type-2 fuzzy PI/PD controller of Takagi–Sugeno type." Engineering Applications of Artificial Intelligence 87 (2020): 103273.

[8] Montazeri-Gh, Morteza, and Shabnam Yazdani. "Application of interval type-2 fuzzy logic systems to gas turbine fault diagnosis." Applied Soft Computing 96 (2020): 106703.

[9] Yip, Chun Ming Tommy, Woei Wan Tan, and Maowen Nie. "On the difference in control performance of interval type-2 fuzzy PI control system with different FOU shapes." Applied Soft Computing 76 (2019): 517-532.

[10] Liao, Qian-Fang, Da Sun, Wen-Jian Cai, Shao-Yuan Li, and You-Yi Wang. "Type-1 and Type-2 effective Takagi-Sugeno fuzzy models for decentralized control of multi-input-multi-output processes." Journal of Process Control 52 (2017): 26-44.

[11] Mohammadzadeh, Ardashir, and Erkan Kayacan. "A non-singleton type-2 fuzzy neural network with adaptive secondary membership for high dimensional applications." Neurocomputing 338 (2019): 63-71.

[12] Ashrafi, Mohammad, Dilip K. Prasad, and Chai Quek. "IT2-GSETSK: An evolving interval Type-II TSK fuzzy neural system for online modeling of noisy data." Neurocomputing 407 (2020): 1-11.

[13] Shahparast, Homeira, and Eghbal G. Mansoori. "Developing an online general type-2 fuzzy classifier using evolving type-1 rules." International Journal of Approximate Reasoning 113 (2019): 336-353.

[14] Zhou, Haibo, and Hao Ying. "Deriving and analyzing analytical structures of a class of typical interval type-2 TS fuzzy controllers." IEEE Transactions on Cybernetics 47, no. 9 (2016): 2492-2503.

[15] Mendel, Jerry M., Robert I. John, and Feilong Liu. "Interval type-2 fuzzy logic systems made simple." IEEE transactions on fuzzy systems 14.6 (2006): 808-821.

[16] Chung, Jun Ho, Jung Min Pak, Choon Ki Ahn, Sung Hyun You, Myo Taeg Lim, and Moon Kyou Song. "Particle filtering approach to membership function adjustment in fuzzy logic systems." Neurocomputing 237 (2017): 166-174.

[17] Klir, George J., Ute St. Clair, and Bo Yuan. Fuzzy set theory: foundations and applications. Prentice-Hall, Inc., 1997.

[18] Pedrycz, Witold. "Why triangular membership functions?." Fuzzy sets and Systems 64, no. 1 (1994): 21-30.

[19] Muhuri, Pranab K., and Amit K. Shukla. "Semi-elliptic membership function: Representation, generation, operations, defuzzification, ranking and its application to the real-time task scheduling problem." Engineering Applications of Artificial Intelligence 60 (2017): 71-82.

[20] Khanesar, Mojtaba Ahmadieh, Mohammad Teshnehlab, Erdal Kayacan, and Okyay Kaynak. "A novel type-2 fuzzy membership function: Application to the prediction of noisy data." In *2010 IEEE International Conference on Computational Intelligence for Measurement Systems and Applications*, pp. 128-133. IEEE, 2010.

[21] Khanesar, Mojtaba Ahmadieh, Erdal Kayacan, Mohammad Teshnehlab, and Okyay Kaynak. "Levenberg marquardt algorithm for the training of type-2 fuzzy neuro systems with a novel type-2 fuzzy membership function." In *2011 IEEE symposium on advances in type-2 fuzzy logic systems (T2FUZZ)*, pp. 88-93. IEEE, 2011..

[22] Kayacan, Erdal, Andriy Sarabakha, Simon Coupland, Robert John, and Mojtaba Ahmadieh Khanesar. "Type-2 fuzzy elliptic membership functions for modeling uncertainty." *Engineering Applications of Artificial Intelligence* 70 (2018): 170-183.

[23] Baklouti, Nesrine, Ajith Abraham, and Adel M. Alimi. "A beta basis function interval type-2 fuzzy neural network for time series applications." *Engineering Applications of Artificial Intelligence* 71 (2018): 259-274.

[24] Liao, T. Warren. "A procedure for the generation of interval type-2 membership functions from data." *Applied Soft Computing* 52 (2017): 925-936.

[25] Ozen, Turhan, and Jonathan M. Garibaldi. "Effect of type-2 fuzzy membership function shape on modelling variation in human decision making." In *2004 IEEE International Conference on Fuzzy Systems (IEEE Cat. No. 04CH37542)*, vol. 2, pp. 971-976. IEEE, 2004.

[26] Miccio, Michele, and Bartolomeo Cosenza. "Control of a distillation column by type-2 and type-1 fuzzy logic PID controllers." *Journal of Process Control* 24, no. 5 (2014): 475-484.

[27] Abdolkarimi, Elahe Sadat, Golnoush Abaei, Ali Selamat, and Mohammad Reza Mosavi. "A hybrid type-2 fuzzy logic system and extreme learning machine for low-cost INS/GPS in high-speed vehicular navigation system." *Applied Soft Computing* 94 (2020): 106447.

[28] Wu, Dongrui, and Jerry M. Mendel. "Recommendations on designing practical interval type-2 fuzzy systems." *Engineering Applications of Artificial Intelligence* 85 (2019): 182-193.

[29] Li, Zhijun, Kamal Mohy El Dine, Chuan Yang, Takahiro Nozaki, Toshiyuki Murakami, Daohui Zhang, Xingang Zhao et al. "2016 IEEE 14th International Workshop on Advanced Motion Control (AMC)."

[30] Sahu, Rabindra Kumar, Sidhartha Panda, and Narendra Kumar Yegireddy. "A novel hybrid DEPS optimized fuzzy PI/PID controller for load frequency control of multi-area interconnected power systems." *Journal of Process Control* 24, no. 10 (2014): 1596-1608.

[31] Ibrahim, Ahmed Abdul, Hai-bo Zhou, Shuai-xia Tan, Chao-long Zhang, and Ji-an Duan. "Regulated Kalman filter based training of an interval type-2 fuzzy system and its evaluation." *Engineering Applications of Artificial Intelligence* 95 (2020): 103867.